Composites Part B 131 (2017) 184–195

Contents lists available at ScienceDirect

Composites Part B

journal homepage: www.elsevier.com/locate/compositesb

Alumina-graphene hybrid filled epoxy composite: Quantitative validation and enhanced thermal conductivity

M. Wasim Akhtar [a], Yun Seon Lee [b], Dong Jin Yoo [c, d], Jong Seok Kim [a, *]

[a] School of Semiconductor and Chemical Engineering, Chonbuk National University, Jeonju 54896, Republic of Korea
[b] Carbon Composite Materials Research Center, Institute of Advanced Composites Material, Korea Institute of Science and Technology (KIST), Chudong-ro 92, Bongdong-eup, Wanju-gun, 565-905 Jeollabuk-do, Republic of Korea
[c] Graduate School, Department of Energy Storage/Conversion Engineering, Hydrogen and Fuel Cell Research Center, Chonbuk National University, Jeonju 54896, Republic of Korea
[d] Department of Life Science, Chonbuk National University, Jeonju 54896, Republic of Korea

ARTICLE INFO

Article history:
Received 14 November 2016
Received in revised form
17 July 2017
Accepted 29 July 2017
Available online 31 July 2017

Keywords:
Polymer-matrix composites (PMCs)
Thermosetting resin
Thermal properties
Surface modification

ABSTRACT

Alumina-graphene hybrid fillers (*Gr*-Al_2O_3) were synthesized and added to the epoxy matrix to improve thermal properties of the epoxy composite. The alumina particles were surface modified with silane coupling agents like 3-Aminopropyl triethoxysilane (*A*-Al_2O_3). 3-Glycidyloxypropyl trimethoxysilane (GPTMS) was used for the surface modification of the graphene (G-Graphene). These modifications on the filler surface help to develop the interface between the fillers and the epoxy matrix, which might help to form the effective 3D thermal conductive networks. The generation of these 3D networks facilitated in reducing the Kapitza resistance and increases the transportation of phonons in the matrix, Furthermore; it improved the integral procedure decomposition temperature (IPDT) and activation energy (E_a) of the composite. Alumina-graphene hybrid filled epoxy composite (*hAG*-Epoxy) with 50 vol% of hybrid filler (*Gr*-Al_2O_3) expressed the considerable improvement in in-plane thermal conductivity and IPDT by ~8.4 and ~3.1 folds in comparison with neat epoxy, respectively. The significant improvement in thermal conductivity was related to the generation of effective 3D thermal conductive pathways formed by 2D graphene and 1D alumina in the composite.

1. Introduction

The perpetual increase in the demand of miniaturizing electronic devices has provoked the problem associated with heat dissipation. It demands the need of highly efficient thermal conductive and thermally stable materials for thermal management applications [1]. The contemporary electronic devices generate a considerable amount of heat during their operation, which requires the proper thermal management for prolonged performance [2]. The proper removal of heat in such devices is a critical factor, for their reliability in electronic and optoelectronic industries. At present, the inquisition for enhancing the thermal conductivity of the thermal interface materials is gaining momentum to achieve reliable materials which effectively deals in heat dissipation, improved thermal interface materials. To address this problem, the heat sinks are traditionally used but they often subject to crack due to thermal fatigue [3].

Polymers are one of the most promising candidates for thermal interface materials due to their low density and low fabrication cost. However, the low thermal conductivities of polymers limit their applications for thermal interface materials. The use of thermally conductive fillers in polymers is common to enhance the thermal properties. Fiber is also used as a thermally conductive filler due to their high aspect ratio and good mechanical properties, although they require a sufficient amount of filler to achieve appropriate thermal properties [4–6]. The inorganic fillers like alumina, aluminum nitride, and boron nitride are used as thermal conductive fillers in polymers [7–10]. However, the high fraction of these fillers (~50–70 vol%) is usually required to achieve the thermal conductivity up to 1–5 W $m^{-1}K^{-1}$at room temperature [11]. The high amount of fillers generally leads the poor mechanical properties of the composite i.e. not suitable for the practical applications, On the other hand, carbon materials could be more efficient and effective as a thermally conductive filler due to their

* Corresponding author.
E-mail address: js-kim@jbnu.ac.kr (J.S. Kim).

http://dx.doi.org/10.1016/j.compositesb.2017.07.067
1359-8368/

Table 1
Physical properties of epoxy and hardener.

Specifications of chemicals	
Epoxy resin "Kukdo YD-128"	
Specific Gravity (25 °C)	1.17
Viscosity (25 °C) [cps]	11,500–13,500
Epoxy Equivalent Weight EEW (g/eq)	184–190
Curing agent (Hardener) "Aliphatic amine modified hardener KH-602"	
Viscosity (cps at 25 °C)	50–250
Total Amine Value (mgKOH/g)	670–730
Use Level (phr)	25 (YD-128 = 186 g/eq))

high thermal conductivity at room temperature, low density, along with good mechanical properties. Graphite [12], carbon fibers [6], carbon black [13], and fullerenes [14] have been used as thermally conductive filler to enhance the thermal conductivity of the polymers. Recently, graphene with 2D structure has gained a potential interest as a thermally conductive filler, due to its outstanding thermal conductivity, low specific gravity, large surface area and high aspect ratio [15,16]. Owing to 2D dimensional structure, graphene forms interconnective bridges and percolating networks that help in phonon transportation. By adding 0.25 wt % of graphene in a polymer matrix, the thermal conductivity has improved up to 0.212 W $m^{-1}K^{-1}$ (~6%) [17]. The thermal conductivity of polystyrene films is improved by the addition of 2 wt % graphene in composite from 0.158 W $m^{-1}K^{-1}$ to 0.413 W $m^{-1}K^{-1}$. Graphene is a suitable choice as a thermally conductive filler to enhance the thermal properties of the composite, however, the synthesis of carbon-based materials, required low-cost processing steps. In addition, the use of high amount of graphene content improves the electrical conductivity, which is normally not required in case of thermal interface materials (TIMs).

Recently the hybridization of filler to improve the thermal properties of the composite is gaining momentum [18–21]. The conductive network of CNT/Bi_2Te_3 hybrid is incorporated in polyethylene which improves the thermal conductivity up to 0.43 W $m^{-1}K^{-1}$ by adding 2.6 vol % CNTs and 5.1 vol % Bi_2Te_3 [22]. A combined multi-walled carbon nanotubes (MWCNTs) and micro-sized silicon carbide with large amount were incorporated in the epoxy matrix to enhance thermal conductivity up to ~ 6 W $m^{-1}K^{-1}$, [18]. The polygonal aluminum nitride and planar boron nitride particles are used to create an optimal thermal conductive path by the packing efficiency and interfacial resistance of the particle. The thermal conductivity is improved to 8.0 W $m^{-1}K^{-1}$ by introducing 80 vol % of the hybrid filler in 1:1 ratio [23] The thermal conductivity is enhanced up to 30% with dense silicon carbide (SiC)-based composites containing up to 20 vol % of graphene nanoplatelets (GNPs). The addition of GNPs improved the thermal conductivity in the in-plane direction [21].

Hybridization of filler is suitable for enhancing the thermal properties of the epoxy composite, however it requires good interface with the polymer matrix. The inappropriate interfacing between fillers and polymers increases the thermal resistance which hinders the transportation of phonons within the matrix. To deal this issue, most of the researchers are focusing on the surface modification of the filler that helps in the formation of an effective

Table 2
Filler content in the epoxy composite and corresponding thermal conductivity values.

Sample	Al_2O_3 content (vol%)	Graphene content (wt%)	In-plane thermal conductivity ($Wm^{-1}.K^{-1}$)
Pristine Al_2O_3-epoxy composite			
PA-Epoxy	10	–	0.280
	20	–	0.344
	30	–	0.402
	40	–	0.488
	50	–	0.620
Silane modified Al_2O_3-Epoxy composite			
AA-Epoxy	10	–	0.648
	20	–	0.725
	30	–	0.894
	40	–	1.033
	50	–	1.230
Non-modified Al_2O_3/Graphene-epoxy			
AG-Epoxy	10	0.5	0.828
Gr = 0.5 wt%	20	0.5	0.949
	30	0.5	1.061
	40	0.5	1.303
	50	0.5	1.410
Non-modified Al_2O_3/Graphene-epoxy			
AG-Epoxy	10	1.0	0.936
Gr = 1.0 wt%	20	1.0	1.003
	30	1.0	1.167
	40	1.0	1.377
	50	1.0	1.469
Hybrid Al_2O_3/Graphene-epoxy			
hAG-Epoxy	10	0.5	0.973
Gr = 0.5 wt%	20	0.5	1.027
	30	0.5	1.205
	40	0.5	1.402
	50	0.5	1.635
Hybrid Al_2O_3/Graphene-epoxy			
hAG-Epoxy	10	1.0	0.976
Gr = 1.0 wt%	20	1.0	1.098
	30	1.0	1.331
	40	1.0	1.572
	50	1.0	1.681
Neat Epoxy	–	–	0.200

thermal conductive networks. The establishment of well-dispersed particles within the matrix is one of the important factors to improves the thermal conduction [24]. The thermal conductivity of silane functionalized graphite filled epoxy composite has improved to 28 folds over the neat epoxy [25]. The result indicates the grafting the silane molecules on the surface of graphite improved the dispersion. In our previous work, OPD-*f*-Graphene showed extraordinary enhancement in thermal properties when introduced in the epoxy matrix. The enhancement in thermal conductivity is recorded up to 13 folds, by just introducing 6 wt % of the functionalized graphene [26]. Therefore, functionalization of particles helps in better dispersion and strong interconnection between filler and matrix, which helps in thermal conduction.

In this paper, we report on surface modification of alumina-graphene hybrid filler and its effect on thermal properties of epoxy composite. The surface modification was achieved through refluxing, which helps strong interconnection between the particles and good interface with the matrix. The surface modified hybrid filler helps in homogeneous dispersion of the filler and develops highly thermal conductive and thermal stable networks, which helps in improving the thermal conductivity of the epoxy composite. The experimental results for thermal conductivity are also in good agreement with Bruggeman's equation for spherical particles with interface layers.

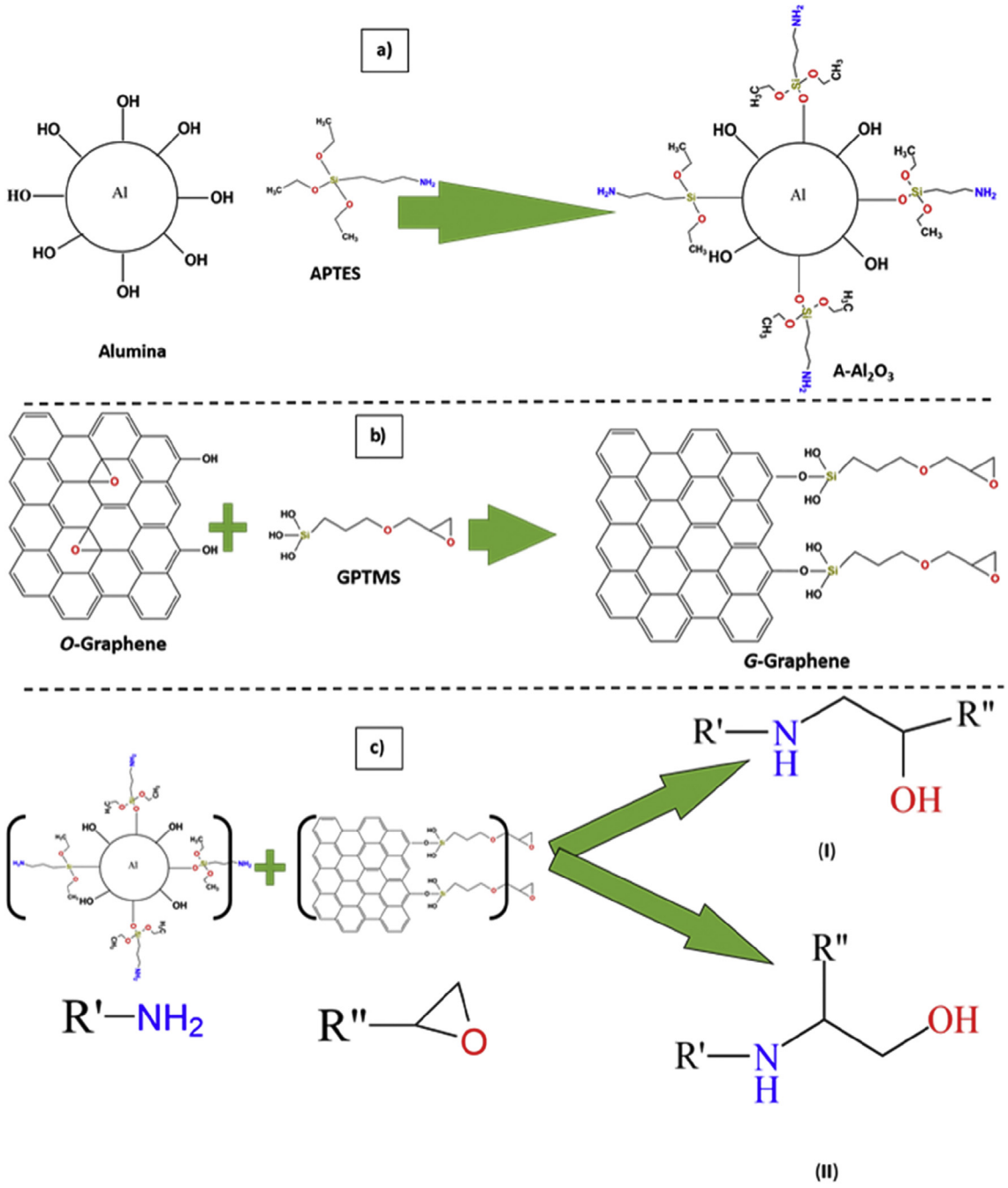

Scheme 1. Schematic illustration of (a) surface modification of alumina with APTES; (b) surface modification of graphene with GPTMS; (c) Hybridization of *A*-Al_2O_3 and *G*-Graphene.

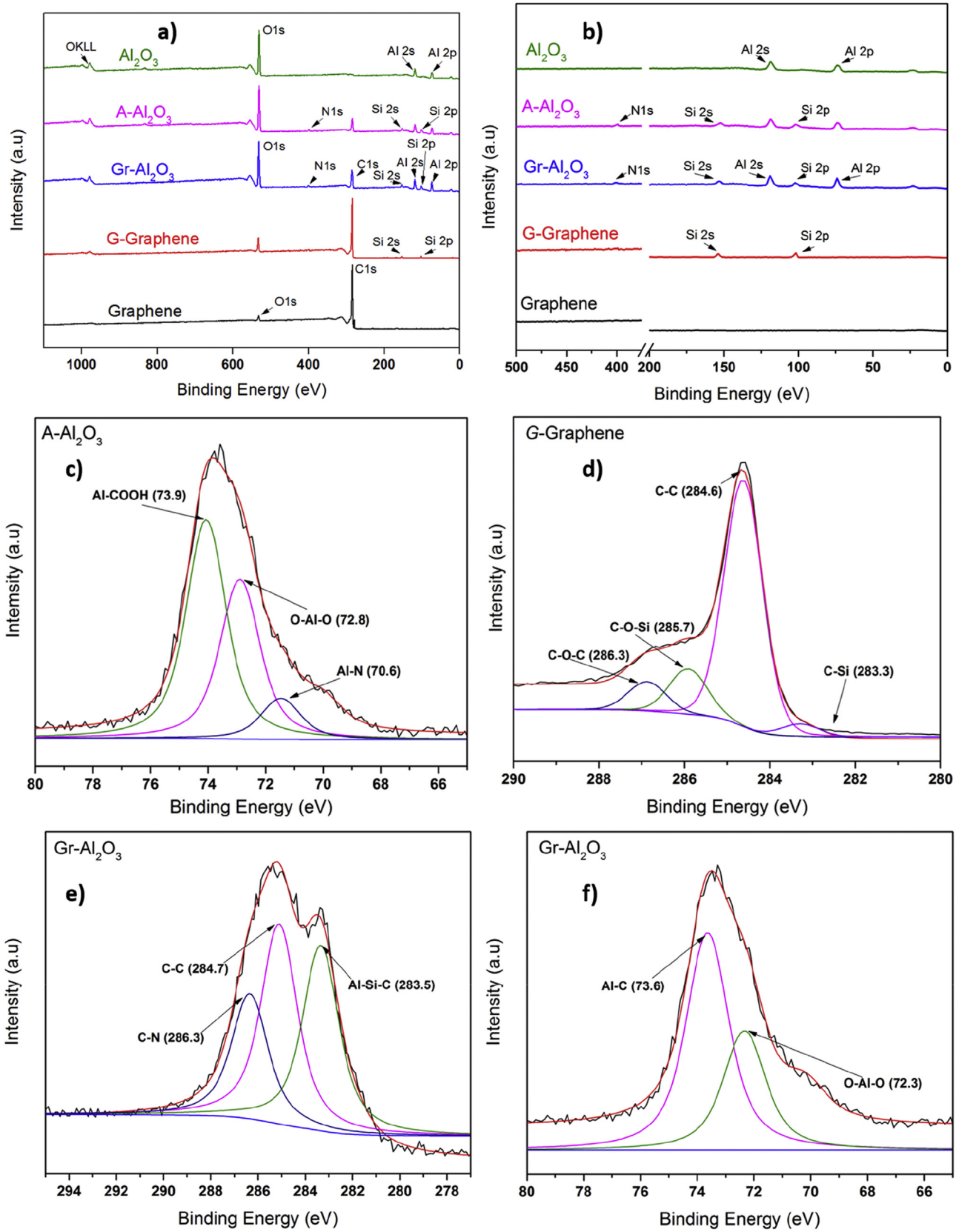

Fig. 1. XPS survey spectra of (a) alumina, graphene and hybrid filler (b) magnified survey spectra of (a). High resolution Al 2p Spectra of A-Al_2O_3 (c); High resolution C 1s Spectra of (d) G-Graphene and (e) Gr-Al_2O_3; (f) Al 2p Spectra of Gr-Al_2O_3.

2. Experimental

2.1. Materials

The epoxy resin based on Diglycidyl ether of bisphenol A (DGEBPA, YD-128) and hardener of modified aliphatic amine (KH-602) were purchased from Kukdo Chem. Co, South Korea. The details of epoxy and hardener are summarized in Table 1. Spherical alumina particles with average size of 4.0 μm were purchased from Sibel Co. Korea Ltd. (South Korea). Graphite powder (<20 μm) and, (3-Aminopropyl) triethoxysilane [APTES] were purchased from Sigma-Aldrich. 3-Glycidoxypropyl trimethoxysilane was obtained from Samchun Chemicals, Korea. 1- Butanol, Sulfuric acid (H_2SO_4, 95%) and Nitric acid (HNO_3, 60%) were purchased from Daejung Chemicals Co. Ltd, Korea. These chemicals were used as received without any purification.

2.2. Surface modification of alumina

The surface treatment of alumina particles was done with 3-aminopropyl triethoxysilane using ethanol with 95% assay and 5% deionized water. In brief, 2 M ethanolic solution of 3-aminopropyl triethoxysilane was first stirred at RT under nitrogen for 12 h. The pH of the reaction mixture was initially adjusted to 4–5 using 4 M acetic acid (5 mL). Finally, 2 g alumina was added to the above reaction mixture and was heated up to 80 °C for further 24 h afterward, the APTES treated alumina particles (A-Al_2O_3) was collected by centrifugation and washed several times with ethanol and hexane to remove unreacted silane. The obtained A-Al_2O_3 was dried under the vacuum at 70 °C.

2.3. Synthesis and surface modification of graphene

Few layers graphene was synthesized through shear exfoliation in 1-Butanol as reported in elsewhere [27]. To attach functional moeity on the graphene surface, the graphene was first mild oxidized (*O*-Graphene) with a 2:6 M of H_2SO_4: HNO_3 in 2-necked round bottom flask. The reactor was placed in a water bath and heated up to 70 °C for 48 h under continuous stirring at 200 rpm followed by filtration and drying under vacuum. Afterward, 50 mL

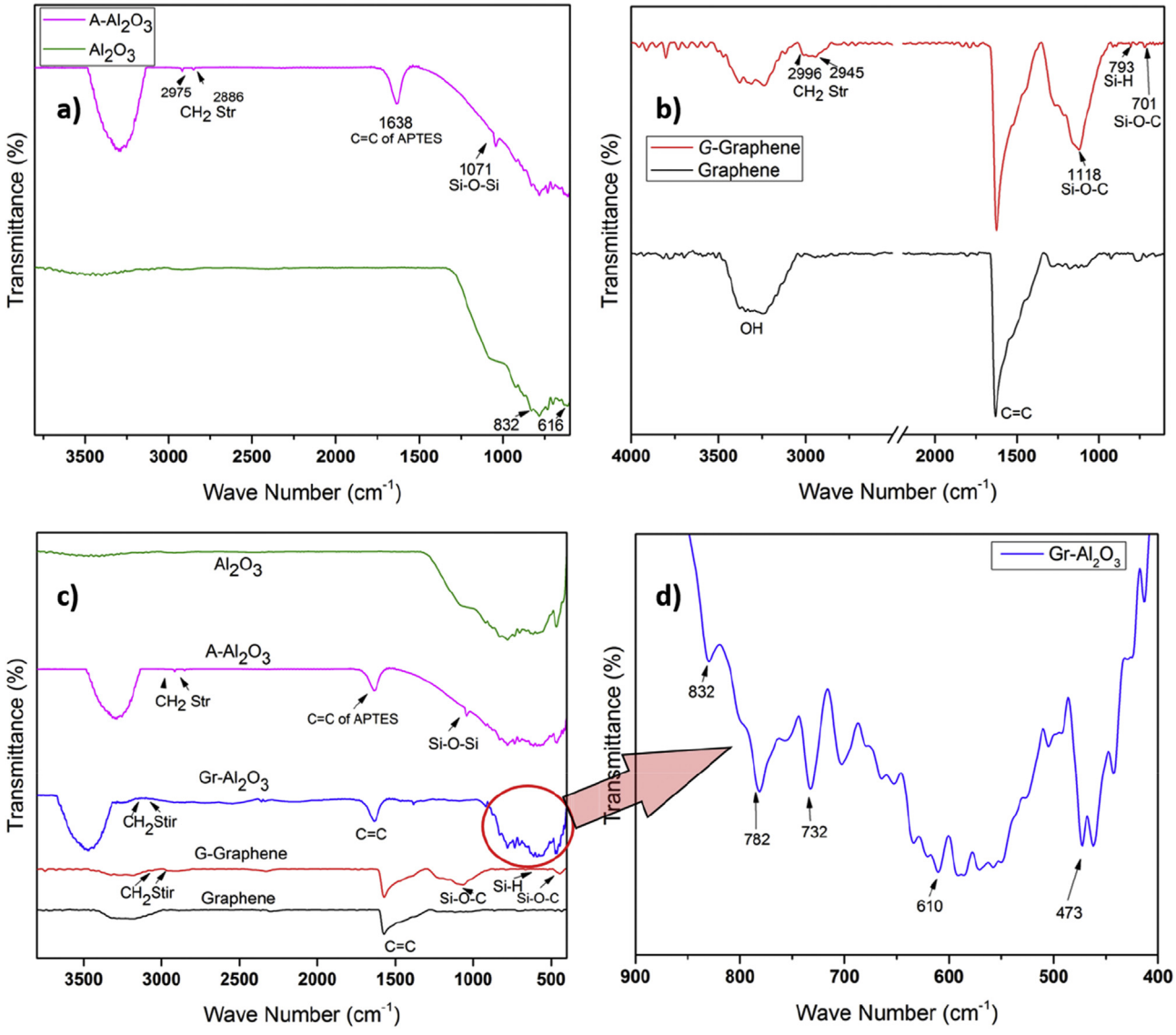

Fig. 2. FTIR spectra of (a) Al_2O and *A*-Al_2O_3; (b) Graphene and *G*-Graphene(c) Combined spectra of fillers (d) magnified spectra of Gr- Al_2O_3.

of 2 M of 3-Glycidoxxypropyl trimethoxysilane in the ethanol-water solvent was hydrolyzed at RT for 12 h. The pH of solvent was maintained ~5 with acetic acid. Finally, 200 mg of *O*-Graphene was added to above reactor and refluxed under 70 °C for 24 h. The final product (G-Graphene) was obtained through centrifugation and washing several times with ethanol and hexane followed by drying under the vacuum.

2.4. Hybridization of A-alumina and G-graphene

The hybridization of alumina with graphene (Gr-Al_2O_3) is achieved through the wet chemical process, In a typical process, 1 g of A-Al_2O_3 was sonicated in 50 mL anhydrous toluene in 2-neck round bottom flask for 15 min, subsequently 10 mg of G-Graphene was added to the mixture. The reactor was heated at 80 °C for 12 h. Finally, the solution was filtered and washed several times with ethanol. The grayish white hybrid filtrate was vacuum dried for overnight.

2.5. Fabrication of epoxy nanocomposite

The hybrid filler (Gr-Al_2O_3) was added to epoxy through centrifugal mixing using Thinky mixer (ARE-310) at 1000 rpm for 15 min, followed by sonication at RT for 30 min. The mixture was degassed under vacuum and then the curing agent was added using mechanical mixing. The weight ratio of epoxy resin with curing agent was fixed to100:25. The hybrid filler contained epoxy composite (hAG-Epoxy) was degassed again to remove the trapped air bubbles and then finally cast into Teflon mold. The mold was heated at 80 °C for 15 min and then cured at room temperature for 48 h. In addition, neat alumina (*NA*-Epoxy), silane modified alumina (*AA*-Epoxy) and non-modified alumina-graphene fillers samples were also used to prepare epoxy composite (*AG*-Epoxy) for comparison of the thermal conductivity. The filler content is listed in Table 2.

2.6. Characterizations

The in-plane thermal conductivity of epoxy thin film (sample dimension: 30 × 05 × 0.3 mm) was characterized by thermal diffusivity analyzer (ULVAC LPIT (Laser-PIT-M2, Japan). Thermal stability was measured by using Thermogravimetric analyzer (TGA-Q50, USA). The surface composition of filler was characterized with X-ray Photoelectron Spectrometer (XPS) System (K-Alpha$^+$, Thermo Scientific, USA). The Fourier transform infrared (FTIR) spectra were measured and analyzed on Fourier transform infrared spectrophotometer (JASCO FT/IR-4100, Japan). Raman scattering was examined on a Raman confocal spectroscopy (Nanofinder®, Japan). The surface morphology and elemental analysis were observed on field emission transmission electron microscopy (FE-SEM) (Carl Zeiss Supra 40VP, Germany).

3. Result and discussion

3.1. Surface modification and characterization of Gr-Al_2O_3 hybrids

Generation of efficient thermal conductive pathways is an important factor in improving the thermal properties of the composite. There is a significant effect of filler geometry on the thermal conductivity of the polymers [28]. The hybridization of various fillers with different dimension and shapes help to create stable conductive networks, which facilitates the conduction of phonons. Hybridization of different fillers is achieved through chemical modification of fillers. In this work; the alumina particles undergo condensation with Al-OH group at the closet particle surface after being treated with silane, as shown in Scheme 1(a). Graphene is first mild oxidize and then silane is attached through refluxing with 3-Glycidoxxypropyltrimethoxysilane (Scheme 1(b)). Scheme 1(c) shows the hybridization mechanism between the surface modified alumina and graphene. The chemical structure of the filler is determined with the X-ray photon spectroscopy (XPS) as shown in Fig. 1. The survey of *A*-Al_2O_3 indicates the presence to silicon and nitrogen, which confirms the modification of alumina with APTES. After surface modification of graphene with GPTMS, the presence of silicon confirms that silane is attached on the graphene. After the hybridization, the survey spectra of hybrid filler (Gr-Al_2O_3) indicate the presence of aluminum (71 eV), silicon (100 eV), carbon (284.6 eV), nitrogen (398 eV) and oxygen (530 eV) (as shown in Fig. 1(a)), which verified the alumina is attached with graphene layers. To examine the surface modification of alumina with APTES, the Al 2p spectra of *A*-Al_2O_3 (Fig. 1(c)) can be deconvoluted into

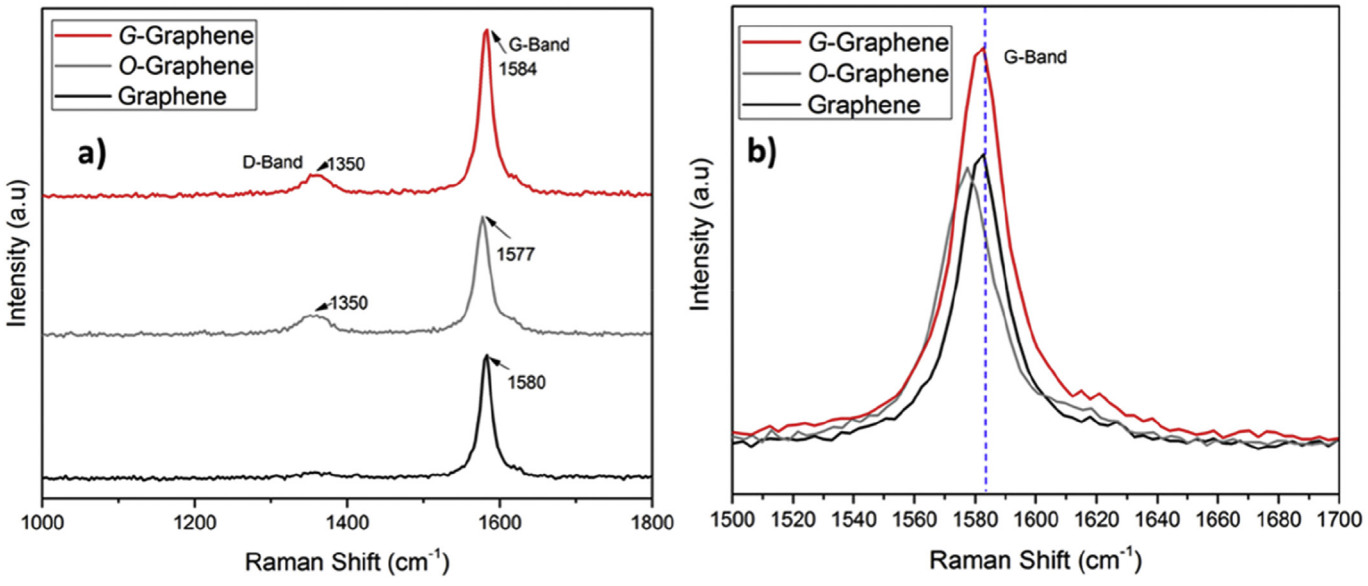

Fig. 3. Raman spectra of (a) Graphene, *O*-Graphene, and *G*-Graphene; (b) G-band of all graphene samples.

three binding energies at 70.6eV, 72.8.6eV and 73.9eV, corresponding to Al-N, Al_2O_3, and -COOH groups, respectively [29,30]. The formation of Al-N and Al-COOH bond confirms the attachment of silane with alumina structure. The C1s spectrum of *G*-Graphene is deconvoluted into four binding energies at 283.3 eV, 284.6 eV, 285.7 eV and 286.3 eV as shown in Fig. 1(c). Fig. 1(d) shows the binding energy at 284.6 eV is due to C-C which is related to non-oxidized graphite structure. The appearance of C-Si (283.3 eV) and C-*O*-Si (285.7 eV), indicates that the GPTMS is grafted on the graphene sheets. This result is consistent with previous literature [31]. The hybridization is further confirm from the C1s spectra of Gr-Al_2O_3 as shown in Fig. 1(e), which is deconvoluted into three different binding energies at 283.5 eV, 284.7 eV and 286.3 eV, are related to C-C (284.7 eV), C-N (286.3 eV) and C-Si-Al (283.5 eV) respectively [32,33]. The appearance of a new peak at 283.6 eV confirms the formation of a bond between alumina and graphene. The appearance of a new peak at 73.6 eV after hybridization in Al 2p spectra of Gr-Al_2O_3 in Fig. 1(d), confirms the attachment of alumina with graphene [34].

The surface modification and interfacing between alumina and graphene were also studied by FTIR spectroscopy. Fig. 2(a) shows the FTIR spectra of unmodified and modified alumina. In comparison with pure alumina, the *A*-Al_2O_3 contain different peaks at 1071 cm^{-1}, 1638 cm^{-1}, 2886 cm^{-1} and 2975 cm^{-1} as shown in Fig. 2(a), which is quite similar to FTIR spectrum of APTES [35]. The peaks at 2886 cm^{-1} and 2975 cm^{-1} are due to absorption of CH_2 groups in aliphatic chain. The peak at 1071 cm^{-1} indicates the Si-*O*-Si asymmetric stretching vibration [36]. The presence of CH_2 and Si-*O*-Si groups reveals the grafting of silane on the surface of alumina. The FTIR spectra of *G*-Graphene, reveals some new peaks at 701 cm^{-1}, 793 cm^{-1}, 1118 cm^{-1}, 2945 cm^{-1} and 2995 cm^{-1} that are not present in Graphene Fig. 2(b). The peaks at 2945 cm^{-1} and 2995 cm^{-1} corresponded to asymmetric vibration of alkyl groups which are associated with silane moieties. The appearance of new peaks at 701 cm^{-1} and 1118 $cm^{-1}$is assigned with Si—O—C, whereas the peak at 793 cm^{-1} in linked with Si-H, which confirms the surface modification of graphene with GPTMS [37]. Fig. 2(c) shows the FTIR spectra of Gr-Al_2O_3 hybrid filler. The peaks at 473 cm^{-1}, 610 cm^{-1}, 732 cm^{-1}, 782 $cm^{-1}$and 832 cm^{-1} are the characteristic peaks of alumina (Fig. 2(d)), which is assigned to vibration of Al-O [38]. The bands at 1640 cm^{-1} are due to the aromatic ring of C=C. The bands at 2890 cm^{-1} and 2985 cm^{-1} are associated with symmetric and asymmetric vibrations of alkyl groups. The presence of all characteristics in Gr-Al_2O_3 spectra further confirms the attachment of alumina with graphene, which is quite comparable with XPS results.

Fig. 3 shows the Raman spectra of graphene, *O*-Graphene, and *G*-Graphene. The G-band and D-band appear at 1580 cm^{-1} and 1350 cm^{-1} respectively. The G-band is due to the E_{2g} phonon at the Brillouin zone center [39] and the D-band is due to the breathing modes of the sp^2 atoms, resulting in the defects at first Brillouin zone [40]. The D-band at 1350 cm^{-1} was observed in Raman spectra of *O*-Graphene, which is due to oxidation of graphene, resulting from the decrease in the size of the in-plane sp^2 domains [41,42]. After functionalization with GPTMS, the G-band in Raman spectra is shifted to 1584 cm^{-1}, indicating the re-emergence of sp^2 carbon network [41]. The degree of defect is related with the intensity ratio of D band and G band. *G*-Graphene has increased I_D/I_G ratio to 0.96 in compare to *O*-Graphene (0.94) due to the generation of the new graphitic domain [43].

3.2. Morphology and dispersion of Gr-Al_2O_3 in epoxy composite

The morphology of hybrid filler (Gr-Al_2O_3) has been investigated to explain the attachment of G-Graphene and A-Al_2O_3 in hybrid filler. Fig. 4 displays the FESEM images of *O*-Graphene and hybrid filler (Gr-Al_2O_3). Fig. 4(a) shows the sheet like morphology of graphene, indicating less aggregation of sheets after surface modification. It is clearly visible in Fig. 4 (b) that large Al_2O_3 particles are attached with thin graphene sheet. At high magnification (Fig. 4(c)), Graphene sheet cover the large Al_2O_3 particle, suggesting the proper attachment of G-Graphene to A-Al_2O_3. Herein, the surface

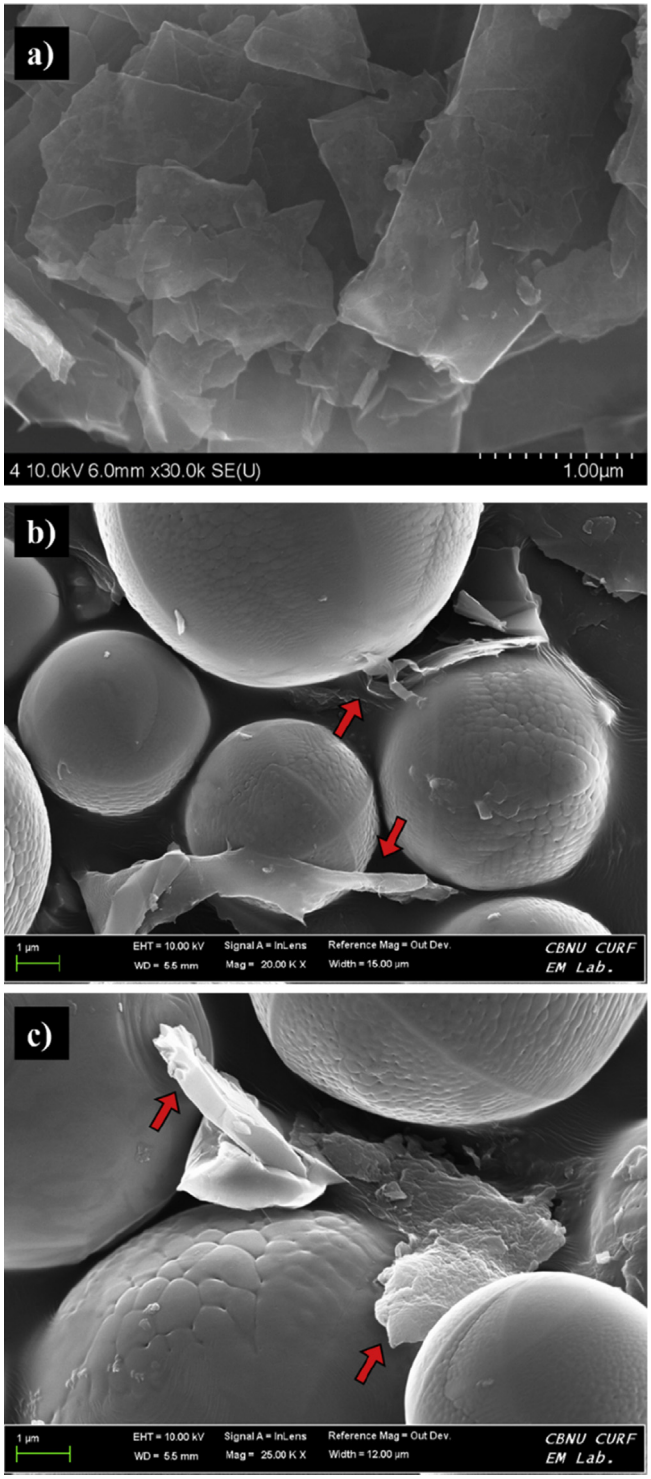

Fig. 4. FESEM images of (a) *O-Graphene*; (b–c) Hybrid alumina-graphene filler (*Gr-Al_2O_3*).

modification of *O*-Graphene and Al_2O_3 is considerably improved the interface properties in hybrid filler which might helpful to enhance the thermal properties of epoxy composite. The morphology of fracture surface for epoxy composite was investigated by FESEM analysis, as shown in Fig. 5. Fig. 5(a) is the fracture surface of neat epoxy, showing the typical fracturing behavior of epoxy resin. Whereas, the epoxy composite presents totally different fracture behavior, as shown in Fig. 5(b–e). The fracture surface to epoxy composite with pristine alumina shows agglomerated particles embedded in epoxy matrix Fig. 5(b). The *A*-Al_2O_3 filler is well dispersed in the epoxy matrix after being treated with silane, as shown in Fig. 5(c). However, the mixture of alumina and graphene filled epoxy composite (*AG*-Epoxy) shows different interfaces due to improper bond between the alumina and graphene (Fig. 5(d)). The fracture morphology of *hAG*-Epoxy display a well-oriented and interconnected alumina-graphene hybrid filler which is evenly dispersed in the epoxy matrix, shown in Fig. 5(e). At high magnification mode (Fig. 5 (h)), the inset shows that the

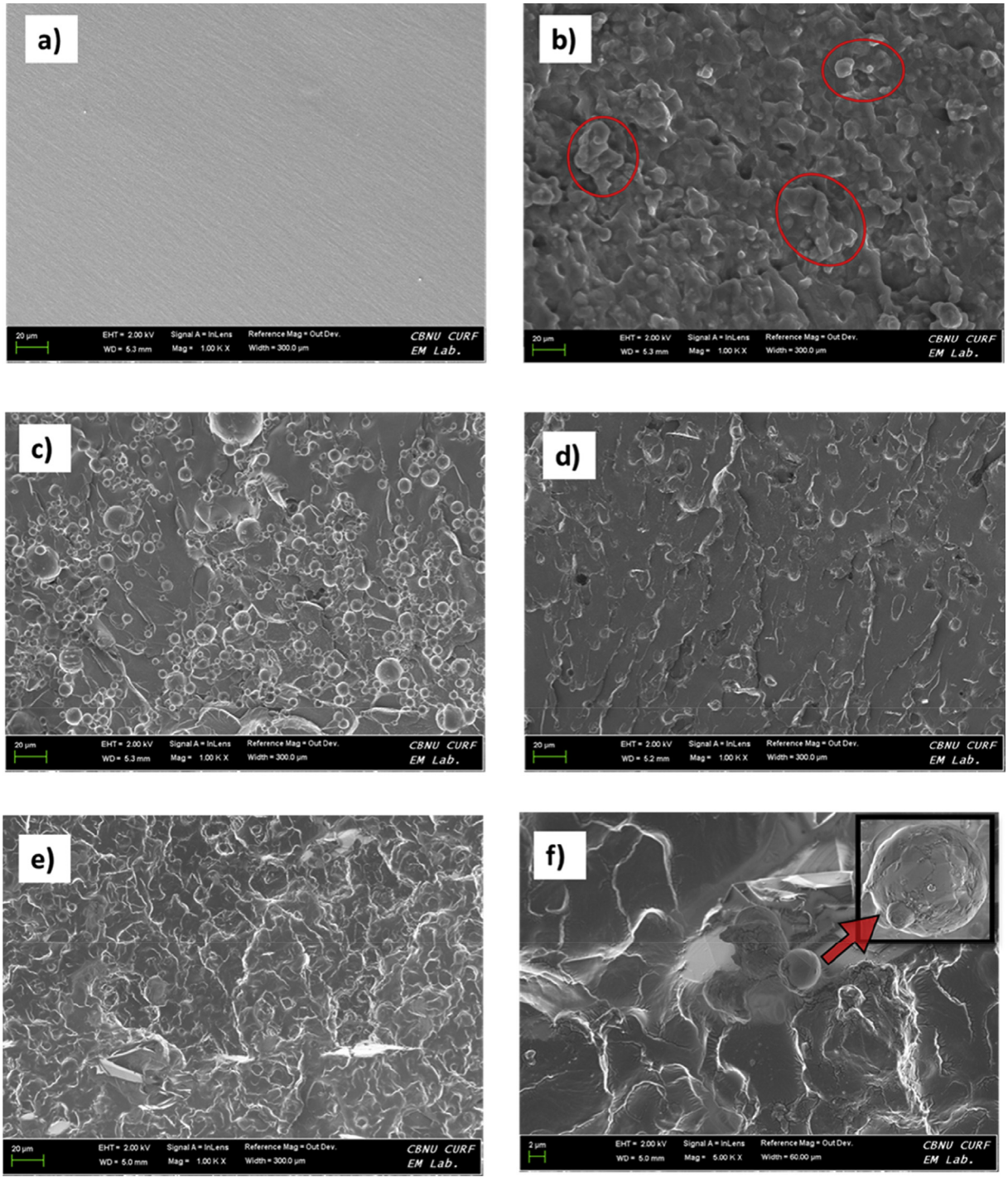

Fig. 5. FESEM images of (a) Neat Epoxy; (b) pristine alumina-filled epoxy (*PA*-Epoxy); (c) silane modified alumina-filled epoxy (*AA*-Epoxy); (d) alumina-graphene filled epoxy (*AG*-Epoxy); (e) Hybrid alumina-graphene filled epoxy (*hAG*-Epoxy); (f) magnified image of *hAG*-Epoxy and inset shows the alumina covered graphene.

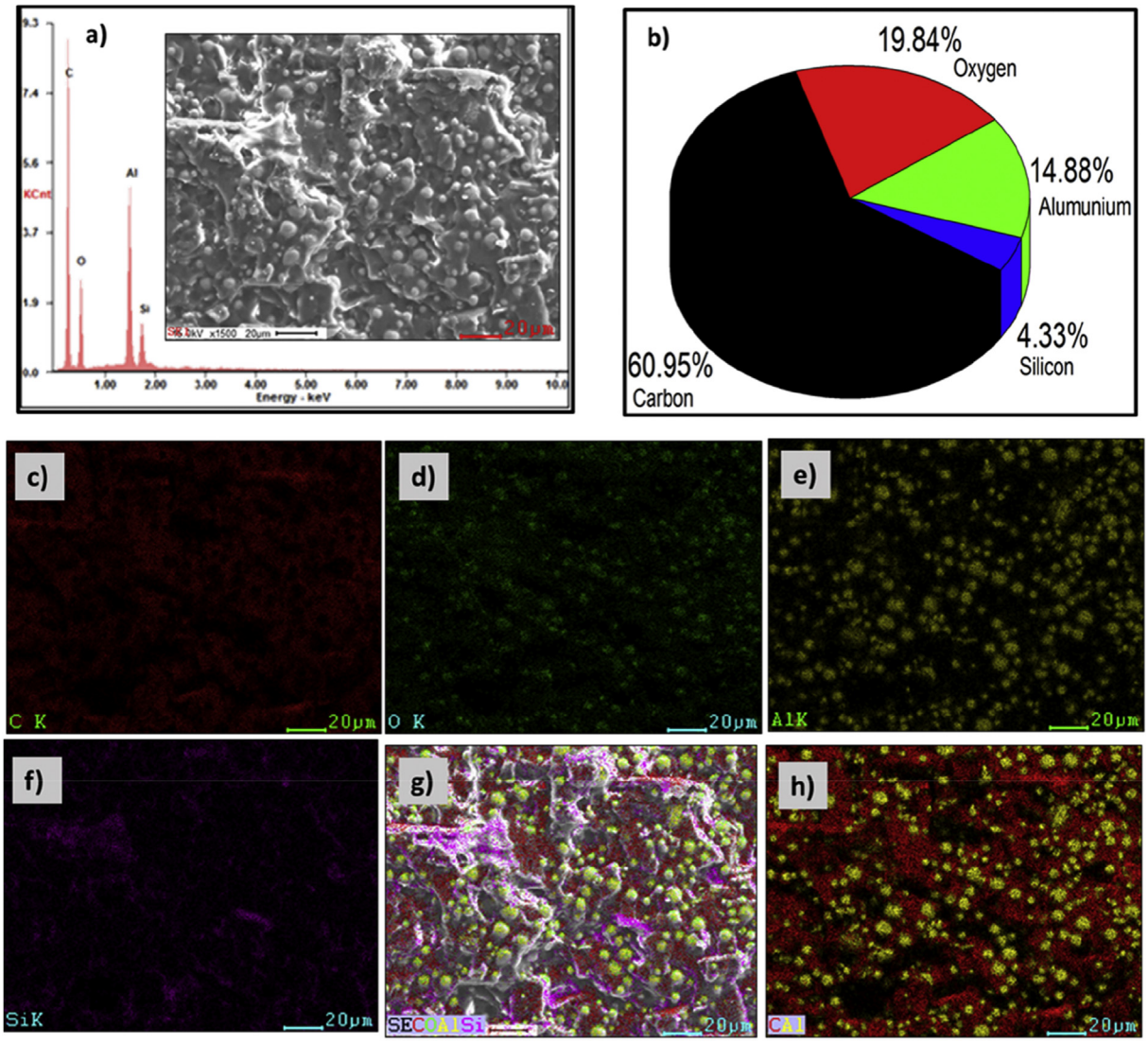

Fig. 6. (a–b) EDX spectra and elemental analysis of *h*AG-Epoxy (*A*-Al_2O_3 = 50 vol %, *G*-Graphene = 1 wt %); (c–f) carbon, oxygen and aluminum and nitrogen mapping image of *h*AG-Epoxy; (g) elemental mapping of C, O, Al & Si; (h) elemental mapping of Al & C.

graphene layers are well surrounded with alumina sphere after the hybridization. It can be seen that the surface modification considerably helps to generate bond between the fillers as well as establishes a strong interface between fillers and matrix. Furthermore, the EDX analysis of *hAG*-Epoxy confirms the presence of silicon and nitrogen, as shown in Fig. 6(a–b). To check the homogeneous dispersion of the filler, the elemental mapping is recorded the location of the elements Fig. 6(c–h). Fig. 6(g) shows that alumina and graphene are well dispersed in the epoxy matrix after hybridization. The mapping images (Fig. 6 (h)) of Al and C reveal interconnection of graphene sheet with alumina particles. Elemental mapping further confirms that surface modification of alumina and graphene could help the filler to uniformly disperse in the epoxy matrix.

3.3. Thermal properties of Gr-Al_2O_3 filled epoxy composite

The thermal stability of the epoxy composite is characterized through Thermogravemetric analysis (TGA), as shown in Fig. 7(a). A prominent weight loss has been observed in the TGA curve due to degradation of epoxy at 300–500 °C [44]. The decomposition temperature in *hAG*-Epoxy has improved up to 58% as compared to neat epoxy. This improvement is related to the introduction of the hybrid filler in the matrix, which enhances the stability of the composite. To further evaluate the thermal stability of the epoxy composites, the thermal stabilities parameters are determined (Table 3). The initial decomposition temperature is determined by using Doyle's Equation [45]. The temperatures of the maximum rate of degradation (T_{max}), and the activation energies for decomposition (E_a), can be used to determine the material life span [46]. The integral procedure decomposition temperature (IPDT) of *hAG*-Epoxy is increased by ~4% as compared to *AG*-Epoxy (20 vol % of alumina and 1 wt % of graphene). This increment is attributed to high cross linking of the epoxy with the hybrid filler.

Horowitz and Metzger model is used to calculate the activation energy for decomposition of cured composites from the integration of TGA curve.

$$\ln\left[\ln(1-\alpha)^{-1}\right] = \frac{Ea\Theta}{RT_{max}^2} \quad (1)$$

where; α is the decomposed fraction, T_{max} the temperature at the

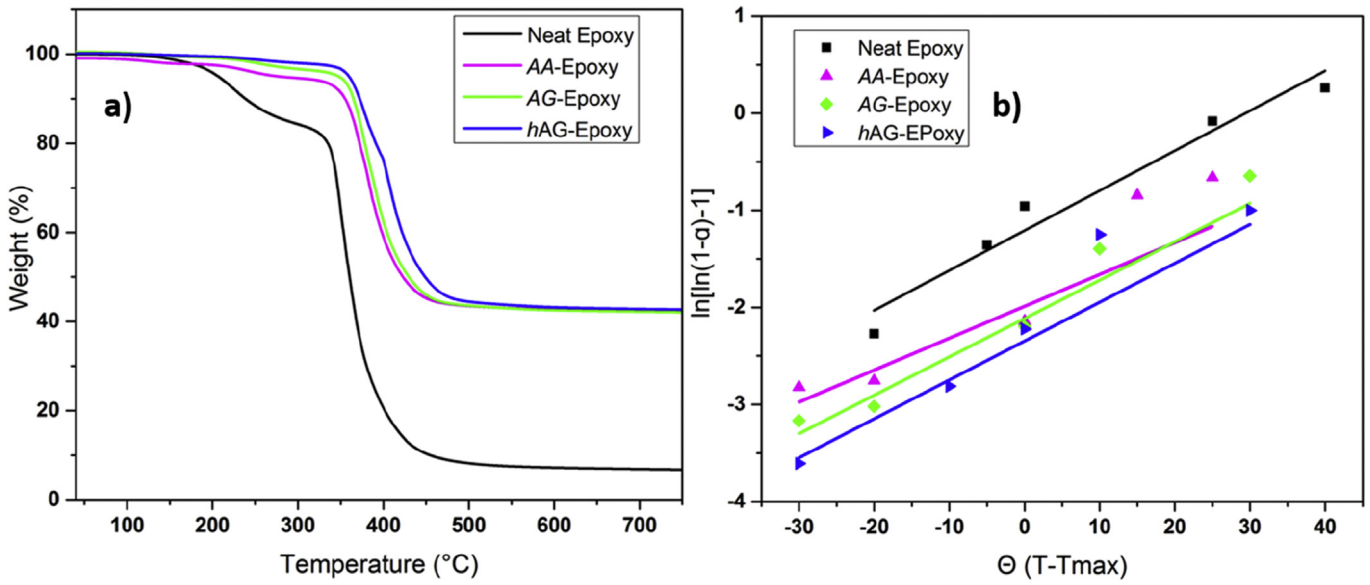

Fig. 7. Thermal stability of epoxy composite, (a) TGA curve of neat epoxy, *AA*-Epoxy, *AG*-Epoxy (Al_2O_3 = 50 vol %, Graphene = 1 wt %) and *hAG*-Epoxy (*A*-Al_2O_3 = 50 vol %, *G*-Graphene = 1 wt %); (b) Plots of ln[ln(1 − α)−1] vs. Θ for neat epoxy, *AA*-Epoxy, *AG*-Epoxy and *hAG*-Epoxy.

Table 3
Thermal stability parameters.

Sample	Filler content alumina (vol %): graphene (wt%)	IPDT (°C)	Ea (KJ/Mol)
Neat Epoxy	–	443.38	82.26
AA-Epoxy	20.0–0.0	1240.11	86.50
AG-Epoxy	20.0–1.0	1358.16	88.82
hAG-Epoxy	20.0–1.0	1408.79	93.88

maximum rate of weight loss, $\theta = T - T_{max}$, and R the gas constant. The graph of ln [ln $(1\text{-}\alpha)^{-1}$] vs. Θ is shown in Fig. 7(b). The activation energy of the composite is determined from slope of the straight line using Eq. (1). The values are listed in Table 3. The E_a of *hAG*-Epoxy and *AG*-Epoxy is estimated 93.88 and 88.82, respectively which is comparatively higher than those of *PA*-Epoxy composite and neat Epoxy. It is quite clear that the activation energy for decomposition is improved after hybridization due to high cross linking and good interface between the particle and the matrix.

Table 2 show the amount of filler content in the epoxy matrix and its corresponding in-plane thermal conductivities values. The thermal conductivity is linearly increasing with the increase of filler content as shown in Fig. 8(a). This enhancement in thermal conductivity might be due to the surface contact of the filler with epoxy interface, which reduces the thermal transport barrier in the composite. In general, thermal conductivity depends on the thermal interface resistance and strong thermal conductive networks. The thermal conductivity of *AA*-Epoxy with 50 vol % of alumina is also improved to ~1.96 folds in comparison with *PA*-Epoxy with similar proportion (Fig. 8(a)), which is related to the strong interconnection between the particle and matrix. Importantly, the 3D alumina-graphene hybrid based epoxy composite shows extraordinary enhancement in the thermal conductivity. While the thermal conductivity of *AG*-Epoxy is increased to 1.46 W m^{-1}. K^{-1} by introducing non-modified mixture of alumina and graphene (A-Al_2O_3 vol % 50, G-Graphene wt % = 1.0), which is ~7.38 folds as compared to neat epoxy. The surface modification further enhances the thermal conductivity up to 1.67 W m^{-1}. K^{-1} in *hAG*-Epoxy with similar fraction of the filler (*A*-Al_2O_3 vol % 50, *G*-Graphene wt % = 1.0). Therefore, the thermal conductivity of *hAG*-Epoxy composite is greatly enhanced by factor of 8.36 as compared to neat epoxy, as shown in Fig. 8(b). The obtained thermal conductivity results are also compared with predicted effective thermal conductive model by using Maxwell and Bruggeman's equation. Maxwell expression is quite comparable with low volume fraction [47]. The predicted thermal conductivities values are calculated by using following Maxwell's equation (2).

$$\frac{K_{eff}}{K_m} = 1 + \frac{3\Phi}{\left(\frac{K_1+2K_m}{K_1+K_m}\right) - \Phi} \tag{2}$$

where; Φ = Volume fraction of the filler, K_1 = thermal conductivity of the filler and K_m = thermal conductivity of the matrix, K_{eff} = Effective thermal conductivity of the composite.

The Maxwell equation is limited to single component of filler and for low volume fraction. Therefore; to quantify more accurate prediction the modified Bruggeman's Model for spherical particles with interface layer has been used [48].

$$\left(\frac{K_m}{K}\right)\left(\frac{K + K_{ps}}{K_{1m} - K_{ps}}\right) = 1 - f \tag{3}$$

Fig. 8(c) shows the comparison, of experimental values and predicted data from theoretical models. It is noted that the obtained thermal conductivity values for *PA*-Epoxy is comparably in good agreement with Maxwell model, however after functionalization, the thermal conductivity of *AA*-Epoxy is considerably enhanced due to the good interface between the filler and matrix. The addition of graphene to alumina in hybrid filler improves the

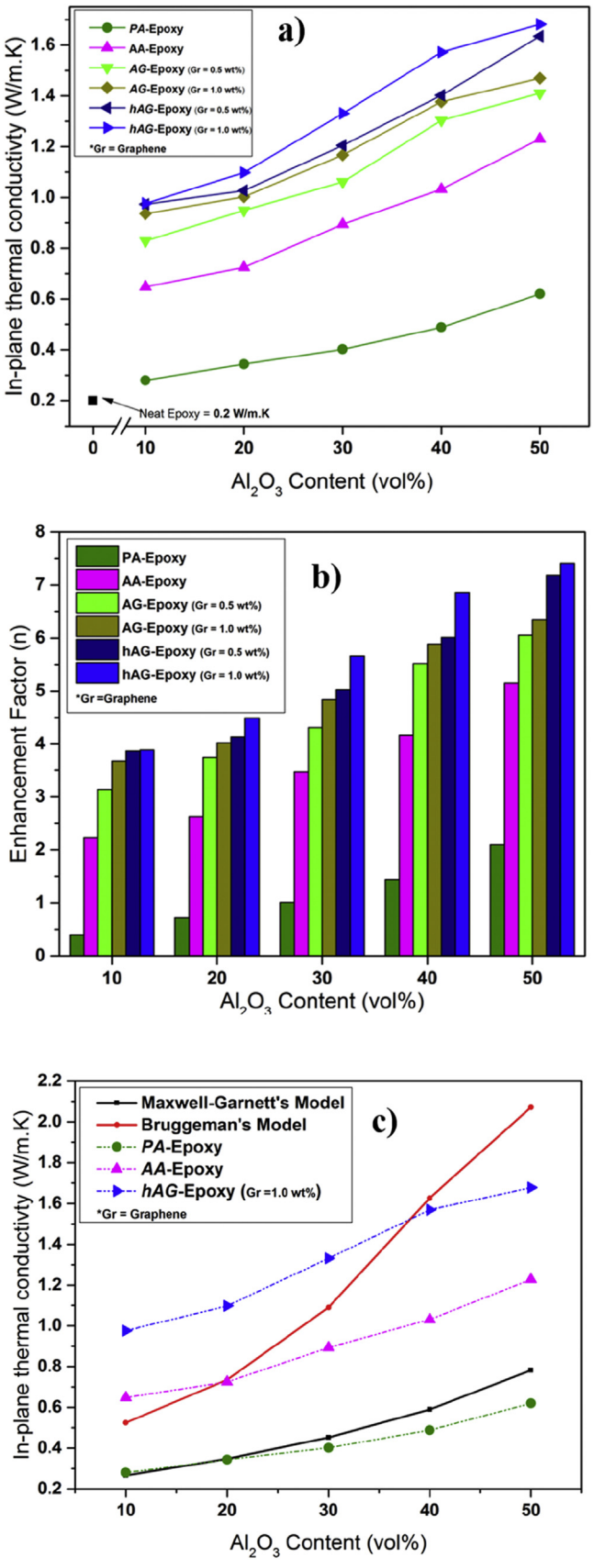

Fig. 8. (a) Thermal conductivity of epoxy composite; (b) Enhancement in thermal conductivity as a function of filler; (c) comparison between numerical predictions and experimental data for thermal conductivity as a function of the volume fraction of fillers.

thermal conductivity and in-plane conductivity of *hAG*-Epoxy is found to be higher in comparison with the predicted values of Bruggeman's Model up to 30 vol % of Al_2O_3. This result is in good agreement with reported work [48]. The comparative data ensures that the surface treatment of the particles helps to create strong interfacial bonding between alumina and graphene, resulting in the creation of effective thermal conductive network with epoxy matrix. Moreover, the 3D structure of hybrid filler might also generate percolating networks that's help the phonons transportation by reducing the thermal interface resistance, resulting in the high thermal conductive and thermally stable epoxy composite.

4. Conclusion

Highly conductive and stable epoxy composite are prepared by the mixing of hybrid fillers of surface modified alumina and graphene. The surface modification of alumina and graphene by silane moieties help to generate good bonding between the fillers and epoxy. The appearance of 3D structure in hybrid filler has improved the interfacial properties with epoxy matrix due to presence of silane moieties. 3D structure in hybrid filler generates compact structure with homogenous distribution of the filler in composite which enhances the phonon transportation by decreasing Kapitza resistance (R_k). The improvement of thermal conductivity is higher than 10 folds for *hAG*-Epoxy (50 vol % *A*-Al_2O_3, 1 wt % *G*–Graphene) in compare to neat epoxy. The thermal stability of *hAG*-Epoxy is also improved and the integral procedure temperature (IPDT) is enhanced to ~3.2 and ~1.1 times to neat epoxy and *AA*-Epoxy; as well as the activation energy for decomposition is elevated to 93.88 kJ mol^{-1} from 82.26 kJ mol^{-1} in compare to neat epoxy. The outstanding thermal properties of developed composites is suitable choice for thermal management and feasible for potential application as a thermal interface materials.

Acknowledgement

We acknowledges the Research Funds of Chonbuk National University, Republic of Korea in 2016.

References

[1] Zhang K, Chai Y, Yuen MMF, Xiao DGW, Chan PCH. Carbon nanotube thermal interface material for high-brightness light-emitting-diode cooling. Nanotechnology 2008;1921. pp.215706.
[2] Viswanath R, Wakharkar V, Watwe A, Lebonheur V. Thermal performance challenges from silicon to systems. 2000.
[3] White SR, Sottos NR, Geubelle PH, Moore JS, Kessler MR, Sriram SR, et al. Autonomic healing of polymer composites. Nature 2001;4096822:794–7.
[4] Patton RD, Pittman Jr CU, Wang L, Hill JR, Day A. Ablation, mechanical and thermal conductivity properties of vapor grown carbon fiber/phenolic matrix composites. Compos Part A Appl Sci Manuf 2002;332:243–51.
[5] Biercuk MJ, Llaguno MC, Radosavljevic M, Hyun JK, Johnson AT, Fischer JE. Carbon nanotube composites for thermal management. Appl Phys Lett 2002;8015:2767–9.
[6] Gharagozloo-Hubmann K, Boden A, Czempiel GJF, Firkowska I, Reich S. Filler geometry and interface resistance of carbon nanofibres: key parameters in thermally conductive polymer composites. Appl Phys Lett 2013;10221. pp.213103.
[7] Choi S, Kim J. Thermal conductivity of epoxy composites with a binary-particle system of aluminum oxide and aluminum nitride fillers. Compos Part B Eng 2013;51:140–7.
[8] Putnam SA, Cahill DG, Ash BJ, Schadler LS. High-precision thermal conductivity measurements as a probe of polymer/nanoparticle interfaces. J Appl Phys 2003;9410:6785–8.
[9] Lee E-S, Lee S-M, Shanefield DJ, Cannon WR. Enhanced thermal conductivity of polymer matrix composite via high solids loading of aluminum nitride in epoxy resin. J Am Ceram Soc 2008;914:1169–74.
[10] Yu C, Zhang J, Li Z, Tian W, Wang L, Luo J, et al. Enhanced through-plane thermal conductivity of boron nitride/epoxy composites. Compos Part A Appl Sci Manuf 2017;98:25–31.
[11] Prasher RS, Chang J-Y, Sauciuc I, Narasimhan S, Chau D, Chrysler G, et al. Nano and micro technology-based next-generation package-level cooling solutions.

Intel Technol J 2005;94.
[12] Fukushima H, Drzal LT, Rook BP, Rich MJ. Thermalconductivity of exfoliated graphite nanocomposites. J Therm Analysis Calorim 2006;851:235–8.
[13] El-Tantawy F, Kamada K, Ohnabe H. In situ network structure, electrical and thermal properties of conductive epoxy resin–carbon black composites for electrical heater applications. Mater Lett 2002:112–26. 561–2.
[14] Dresselhaus MS, Dresselhaus G, Eklund PC. Science of fullerenes and carbon nanotubes: their properties and applications. Academic press; 1996.
[15] Balandin AA. Thermal properties of graphene and nanostructured carbon materials. Nat Mater 2011;108:569–81.
[16] Stankovich S, Dikin DA, Dommett GHB, Kohlhaas KM, Zimney EJ, Stach EA, et al. Graphene-based composite materials. Nature 2006;4427100:282–6.
[17] Verdejo R, Barroso-Bujans F, Rodriguez-Perez MA, Antonio de Saja J, Lopez-Manchado MA. Functionalized graphene sheet filled silicone foam nanocomposites. J Mater Chem 2008;1819:2221–6.
[18] Zhou T, Wang X, Liu X, Xiong D. Improved thermal conductivity of epoxy composites using a hybrid multi-walled carbon nanotube/micro-SiC filler. Carbon 2010;484:1171–6.
[19] Goyal V, Balandin AA. Thermal properties of the hybrid graphene-metal nano-micro-composites: applications in thermal interface materials. Appl Phys Lett 2012;1007. pp.073113.
[20] Huang Y, Su Y, Guo X, Guo Q, Ouyang Q, Zhang G, et al. Fabrication and thermal conductivity of copper coated graphite film/aluminum composites for effective thermal management. J Alloys Compd 2017;711:22–30.
[21] Román-Manso B, Chevillotte Y, Osendi MI, Belmonte M, Miranzo P. Thermal conductivity of silicon carbide composites with highly oriented graphene nanoplatelets. J Eur Ceram Soc 2016;3616:3987–93.
[22] Pang H, Piao Y-Y, Tan Y-Q, Jiang G-Y, Wang J-H, Li Z-M. Thermoelectric behaviour of segregated conductive polymer composites with hybrid fillers of carbon nanotube and bismuth telluride. Mater Lett 2013;107:150–3.
[23] Hong J-P, Yoon S-W, Hwang T, Oh J-S, Hong S-C, Lee Y, et al. High thermal conductivity epoxy composites with bimodal distribution of aluminum nitride and boron nitride fillers. Thermochim Acta 2012;537:70–5.
[24] Ramanathan T, Abdala AA, Stankovich S, Dikin DA, Herrera-Alonso M, Piner RD, et al. Functionalized graphene sheets for polymer nanocomposites. Nat Nano 2008;36:327–31.
[25] Ganguli S, Roy AK, Anderson DP. Improved thermal conductivity for chemically functionalized exfoliated graphite/epoxy composites. Carbon 2008;465:806–17.
[26] Akhtar MW, Lee YS, Yang CM, Kim JS. Functionalization of mild oxidized graphene with O-phenylenediamine for highly thermally conductive and thermally stable epoxy composites. RSC Adv 2016;6102:100448–58.
[27] Wasim Akhtar M, Park CW, Kim YS, Kim JS. Facile large scale production of few-layer graphene sheets by shear exfoliation in volatile solvent. J Nanosci Nanotechnol 2015;1512:9624–9.
[28] Chauhan D, Singhvi N, Singh R. Effect of geometry of filler particles on the effective thermal conductivity of two-phase systems. Int J Mod Nonlinear Theory Appl 2012;102. pp.40.
[29] DeKoven BM, Hagans PL. XPS studies of metal/polymer interfaces — thin films of Al on polyacrylic acid and polyethylene. Appl Surf Sci 1986;272:199–213.
[30] Waldrop JR, Grant RW. Measurement of AlN/GaN (0001) heterojunction band offsets by X-ray photoemission spectroscopy. Appl Phys Lett 1996;6820:2879–81.
[31] Wan Y-J, Gong L-X, Tang L-C, Wu L-B, Jiang J-X. Mechanical properties of epoxy composites filled with silane-functionalized graphene oxide. Compos Part A Appl Sci Manuf 2014;64:79–89.
[32] Pu X, Zhang H-B, Li X, Gui C, Yu Z-Z. Thermally conductive and electrically insulating epoxy nanocomposites with silica-coated graphene. RSC Adv 2014;429:15297–303.
[33] Waldrop JR, Grant RW. Formation and Schottky barrier height of metal contacts to β-SiC. Appl Phys Lett 1990;566:557–9.
[34] Maruyama B, Ohuchi FS, Rabenberg L. Catalytic carbide formation at aluminium-carbon interfaces. J Mater Sci Lett 1990;97:864–6.
[35] Su F, Lu C, Kuo S-C, Zeng W. Adsorption of CO_2 on amine-functionalized Y-type zeolites. Energy & Fuels 2010;242:1441–8.
[36] Huang A, Wang N, Caro J. Seeding-free synthesis of dense zeolite FAU membranes on 3-aminopropyltriethoxysilane-functionalized alumina supports. J. Membr. Sci. 2012;389:272–9.
[37] Lee CY, Le QV, Kim C, Kim SY. Use of silane-functionalized graphene oxide in organic photovoltaic cells and organic light-emitting diodes. Phys Chem Chem Phys 2015;1714:9369–74.
[38] Vázquez A, López T, Gómez R, Bokhimi, Morales A, Novaro O. X-ray diffraction, FTIR, and NMR characterization of sol–gel alumina doped with lanthanum and cerium. J Solid State Chem 1997;1282:161–8.
[39] Tuinstra F, Koenig JL. Raman spectrum of graphite. J Chem Phys 1970;533:1126–30.
[40] Ferrari AC, Robertson J. Interpretation of Raman spectra of disordered and amorphous carbon. Phys Rev B 2000;6120:14095–107.
[41] Kudin KN, Ozbas B, Schniepp HC, Prud'homme RK, Aksay IA, Car R. Raman spectra of graphite oxide and functionalized graphene sheets. Nano Lett 2008;81:36–41.
[42] Ferrari AC, Meyer JC, Scardaci V, Casiraghi C, Lazzeri M, Mauri F, et al. Raman spectrum of graphene and graphene layers. Phys Rev Lett 2006;9718. pp.187401.
[43] Stankovich S, Dikin DA, Piner RD, Kohlhaas KA, Kleinhammes A, Jia Y, et al. Synthesis of graphene-based nanosheets via chemical reduction of exfoliated graphite oxide. Carbon 2007;457:1558–65.
[44] Park S-J, Jin F-L. Thermal stabilities and dynamic mechanical properties of sulfone-containing epoxy resin cured with anhydride. Polym Degrad Stab 2004;863:515–20.
[45] Doyle CD. Series approximations to the equation of thermogravimetric data. Nature 1965;2074994:290–1.
[46] Park S-J, Jin F-L, Lee J-R. Synthesis and thermal properties of epoxidized vegetable oil. Macromol Rapid Commun 2004;256:724–7.
[47] Pietrak K, Wisniewski TS. A review of models for effective thermal conductivity of composite materials. J Power Technol 2015;951. pp.14.
[48] Ordóñez-Miranda J, Alvarado-Gil JJ, Medina-Ezquivel R. Generalized bruggeman formula for the effective thermal conductivity of particulate composites with an interface layer. Int J Thermophys 2010;314:975–86.